

Controllable Morphology Evolution and Photoluminescence of ZnSe Hollow Microspheres

Baoyou Geng,^{*,†} Jiahui You,[†] Fangming Zhan,[†] Mingguang Kong,[‡] and Caihong Fang[†]

College of Chemistry and Materials Science, Anhui Key Laboratory of Functional Molecular Solids, Anhui Normal University, Wuhu 241000, People's Republic of China, and Institute of Solid State Physics, Chinese Academy of Sciences, Hefei 230031, People's Republic of China

Received: April 23, 2008; Revised Manuscript Received: May 16, 2008

Hollow ZnSe microspheres were successfully synthesized by a simple chemistry vapor deposition method in a horizontal tube furnace. The as-obtained samples were characterized by X-ray diffraction, field emission scanning electron microscopy, transmission electron microscopy, and energy-dispersive X-ray spectrometry. The growth mechanism of the ZnSe microspheres was discussed in detail, which can be addressed as the SO₂ gas trap, expand, and burst during the deposition process. The morphology evolutions of the microspheres were observed. The size, open mouth, surface state, and morphology of the hollow ZnSe microspheres could be adjusted through changing the experimental conditions. Photoluminescence measurements show that the as-synthesized hollow ZnSe microspheres exhibit strong blue emissions with the intensities being adjustable. These hollow ZnSe microspheres may have promising applications in blue emitters, gas sensors, microreactors, and catalyst carriers.

Introduction

ZnSe, which has a well-known wide, direct bandgap ($E_g = 2.7$ eV) semiconductor material, is a potentially good material for short-wavelength photoelectronic devices, including blue laser diodes (LDs), light-emitting diodes (LEDs), photodetectors, high-density optical storage, and full-color displays.^{1–9} Controlling the size and dimensions of ZnSe may lead to further novel properties. In recent years many groups have synthesized all kinds of morphology of ZnSe with many methods, for example, wires and ribbons,^{10–14} rods,^{15–18} sheets,^{19,20} core/shell,^{21,22} hollow spheres,^{23,24} etc. With the increasing development of science and technology, the inorganic material hollow spheres have shown a promising perspective in many fields, such as catalysts, dyes or inks, coatings, filters, and microreactors for their low densities, high surface areas, and unique optical, electrical, and surface properties.^{25–27} The production of hollow spheres of inorganic materials can be achieved via a number of methods, including nozzle-reactor systems, emulsion/water extraction techniques, template method, or hydrothermal.^{28–33} The methods mentioned above are mainly focused on solution and template, which result in the complication of preparation. In the solution environments, the conditions including temperature, pH value, solvents, ionic strength, etc., which are hard to control exactly, and the reaction are easily overcome, whereas the template methods are extremely complicated, time-consuming, and often break the hollow sphere during template removal. Therefore, how to fabricate the hollow ZnSe spheres by controlling size and morphology is still a challenge.

In this paper, we develop a simple chemistry vapor deposition (CVD) route to fabricate the ZnSe hollow microspheres, which have a remarkable photoluminescence (PL) property. The intensity of the PL spectra can be adjusted through changing the experimental conditions. The growth mechanism of the ZnSe microspheres is discussed in detail, which can be addressed as

SO₂ gas trap, expand, and burst during the deposition process. More important, the morphology evolutions of the as-prepared microspheres are observed. The size, open mouth, surface state, and morphology of the hollow ZnSe microspheres can be adjusted through changing the experimental conditions. These hollow ZnSe microspheres may have promising applications in blue emitters, gas sensors, microreactors, and catalyst carriers due to their unique hollow structure.

Experimental Section

To synthesize the ZnSe hollow microstructures, a Si (100) substrate (5 mm × 10 mm) was used. The substrate was cleaned in a solution of Piranha (98% H₂SO₄:30% H₂O₂ = 3:1, volume ratio) and ethanol by ultrasonication 20 min and rinsed in deionized water. An alumina boat containing 0.5 g of zinc oxide powder (self-made), 0.6 g of zinc sulfide (self-made), 1.2 g of Se powder (AR, SCRC. Lid), and the substrate, with a downstream separation of 15 cm, was inserted into a horizontal alumina tube with an inner diameter of 20 mm and a heating zone of 200 mm. Prior to heating, the system was flushed with high purity argon (99.999%) for 2 h to eliminate O₂ and pumped down to 5×10^{-2} Torr. Then an Ar flow of 50 standard cubic centimeters per minute (sccm) was used as the carrier gas. The furnace was heated to the reaction temperature of 1100 °C (or 1000 °C) in 30 min and maintained there for period of time. After reaction, the alumina tube was cooled to room temperature under Ar at a flow rate of 50 sccm. The substrate surface appeared to be a layer of gray material.

The phase purity of the as-synthesized products was characterized by X-ray powder diffraction (XRD), which was carried out on an XRD-6000 (Japan) X-ray diffractometer with Cu K α radiation ($\lambda = 1.54060$ Å) at a scanning rate of 0.05 deg·s⁻¹. The morphology and structure were characterized by a field emission scanning electron microscope (FESEM, Hitachi S-4800), a transmission electron microscope (TEM, JEM 2010 F), and an energy-dispersive X-ray spectroscopy (EDS) attached to the TEM. For the TEM observation, the products were dispersed by sonication in alcohol, and the obtained solution was dripped

* Corresponding author. E-mail: bygeng@mail.ahnu.edu.cn.

[†] Anhui Normal University.

[‡] Institute of Solid State Physics.

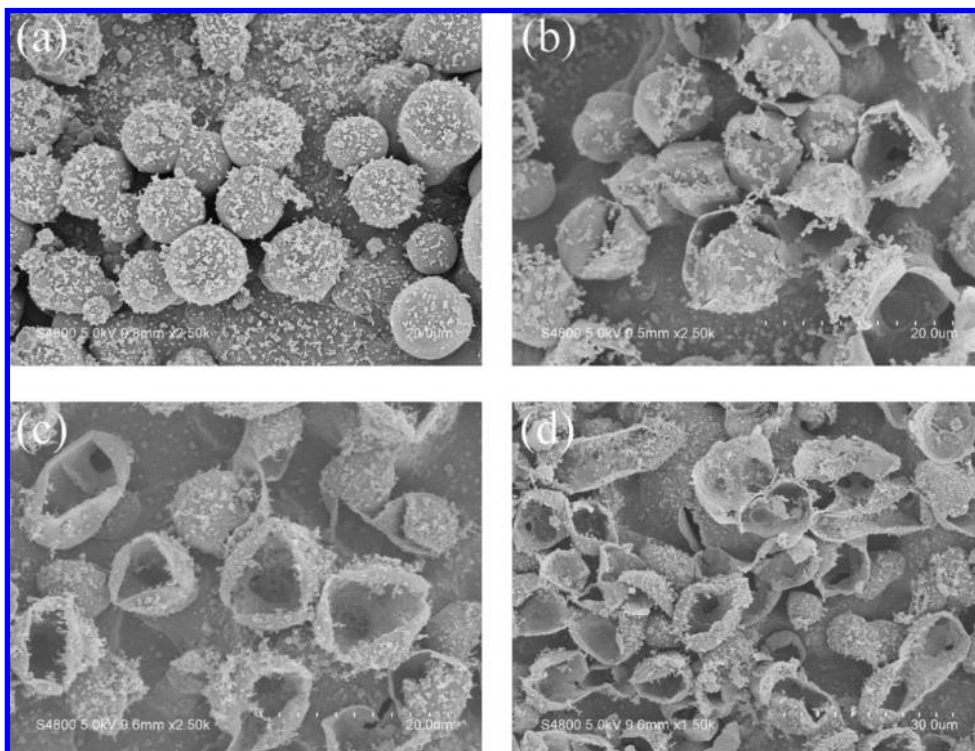


Figure 1. The different morphology of products: (a) complete hollow microspheres; (b) small open mouth hollow microspheres; (c) half open mouth hollow microspheres; and (d) broken mouth hollow microspheres.

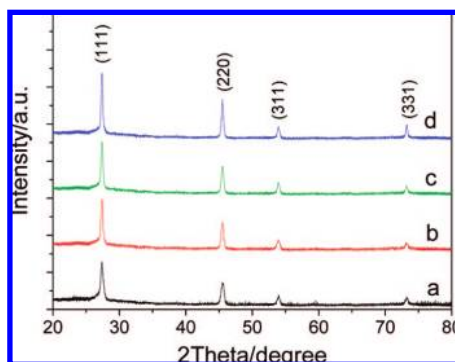


Figure 2. A typical XRD pattern of the as-synthesized ZnSe hollow microspheres: (a) complete hollow microspheres; (b) small open mouth hollow microspheres; (c) half open mouth hollow microspheres; and (d) broken mouth hollow microspheres.

on the TEM copper mesh. Photoluminescence (PL) experiments were carried out on a FLS 920 fluorescence spectrophotometer.

Results and Discussion

The general morphologies of the obtained products are shown in Figure 1a–d. It can be seen that large quantities of hollow microspheres are formed on the Si substrate. The morphology evolves from complete hollow microspheres to broken mouth hollow microspheres with different times and temperatures of reaction. There are also some ZnSe particles on the surface of the hollow microspheres. The SEM images of the hollow microspheres show that the diameters of the hollow microspheres are ca. from 5 to 15 μm .

X-ray diffraction (XRD) analysis was used to determine the phase purity of the microspheres. The corresponding XRD patterns of the products in Figure 1 are shown in Figure 2, which reveals that the peaks of the XRD patterns are identified to originate from (111), (220), (311), and (331); all of the peaks

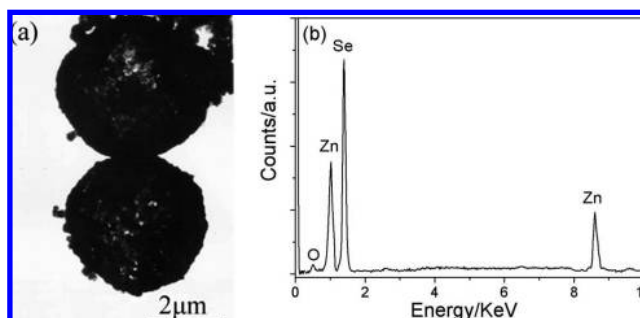


Figure 3. (a) Low-magnification TEM image of the ZnSe hollow microspheres; (b) EDX spectrum from one of the ZnSe hollow microspheres.

can be well indexed to the face-centered cubic ZnSe, with lattice constants of $a = 5.63$, which is in good agreement with the reported data ($a = 5.633$, in the JCPDS file, No. 70-0777).

A low-magnification transmission electron microscopy (TEM) image (Figure 3a) of the typical microspheres after sonication shows the hollow nature of the microspheres. Energy-dispersive X-ray spectrometry (EDS) was also used to determine the local chemical composition of the product. A typical EDS spectrum (Figure 3b) indicates that the products mainly consisted of Zn and Se, which confirms that the products are ZnSe. A relatively weak oxygen peak in the spectrum probably originates from the unavoidable surface adsorption of oxygen onto the samples from exposure to air during sample processing since this material exhibits a high surface-to-volume ratio. The quantification of the peaks gives a ZnSe ratio of about 1:1, which is close to the stoichiometry of ZnSe.

For a complete view of the formation process of the ZnSe hollow microspheres and their growth mechanism, a time-dependent morphology evolution study was conducted. Figure 4a–d shows the morphology evolution of the products obtained at different deposition times at 1100 $^{\circ}\text{C}$. As shown in Figure

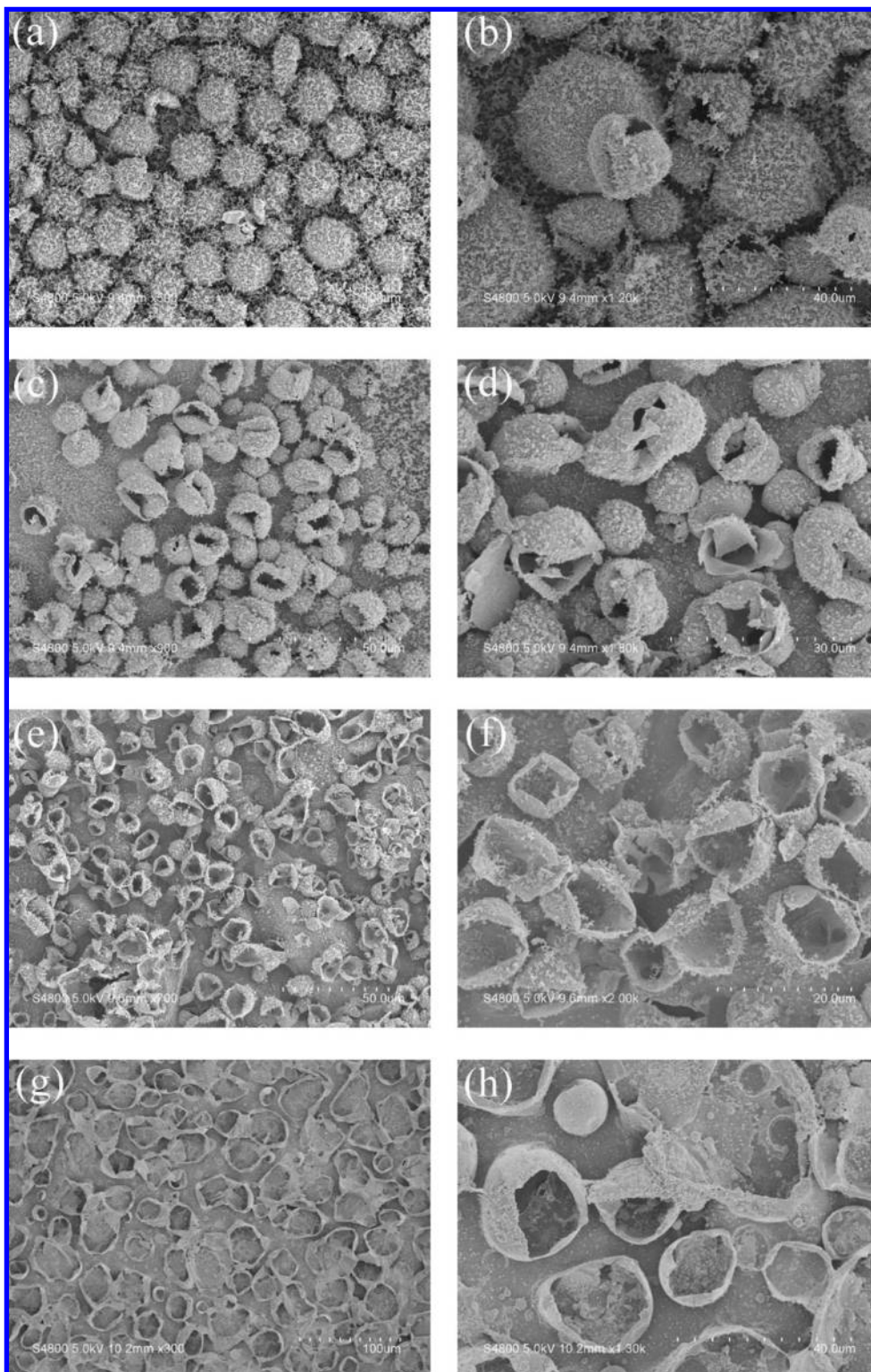
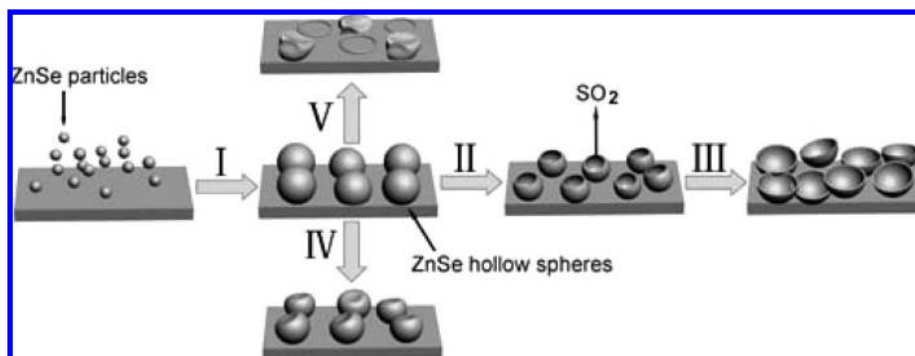


Figure 4. The morphologies of products with different deposition time at 1100 °C: (a and b) 30 min; (c and d) 45 min; (e and f) 60 min; and (g and h) 120 min.

4a, when the deposition time is 30 min, the obtained products are nearly integrated microspheres. Figure 4b shows the high-magnification SEM image of Figure 4a, which reveals that the products are microspheres, and some broken spheres demonstrate that the obtained microspheres should be hollow. In addition, we also found that the surface of the spheres is not smooth with many particles on it. Figure 4c shows the products with a deposition time of 45 min. It shows that the products are hollow spheres with more spheres being broken. The

corresponding high-magnification images (Figure 4d) further reveal the above results. It should be noted that there are still some unbroken spheres among the products and the surfaces of the spheres are slight smoother than those of the spheres in parts a and b of Figure 4.

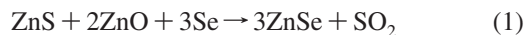
Figure 4e shows the SEM images of the products with a deposition time of 60 min, which reveals that the products are nearly half-hollow spheres with hardly any unbroken spheres found among them. The corresponding high-magnification image

SCHEME 1: A Schematic Illustration of the Process for the Formation of ZnSe Hollow Microspheres

(Figure 4f) shows that the surface of the spheres is much smoother than those of the spheres in Figure 4c,d. When the deposition time was longer, such as 120 min, the morphology of the spheres is evolved further. As shown in Figure 4g, we can see that the open mouth of the hollow spheres enlarged as the deposition time increased and some hollow spheres connected to each other. The corresponding high magnification is shown in Figure 4h, which reveals that some hollow spheres lose more than half-shell. In addition, parts g and h of Figure 4 also show that much fewer particles can be found on the surface of the products than those of the above products. It is obvious that as the deposition time increase, a more enlarged mouth of the hollow spheres is obtained and the surface of the hollow spheres becomes smoother and smoother.

For a better understanding of the growth model, we suggest that the following aspects should be addressed (as shown in Scheme 1).

First, the formation of the ZnSe might be illustrated by the following reaction:



According to the reaction 1, ZnS, ZnO, and Se powders react with each other to form ZnSe clusters accompanied by the release of SO₂ gas when the system is heated to a certain temperature. The ZnSe clusters are carried onto the Si substrate downstream by flowing Ar, and then deposited on the Si substrate, forming nanometer-sized ZnSe particles on the Si substrate, which is at a lower temperature. The existence of SO₂ vapor in the process ensures that small nanoparticles can be obtained, because only a small amount of ZnSe gas is precipitated from the supersaturated gas downstream, which is similar to the situation in the formation of SnO₂/SiO₂ nanorings.³⁴ Second, the melting point of the nanoscale materials will be lower than that of the bulk. During the heating, ZnSe nanoparticles become soft and then fuse together. Meanwhile, SO₂ present in the space between nanoparticles will combine and be trapped inside the newly formed large ZnSe particles as SO₂ bubbles. When the reaction is over and the temperature declines, the vapor is eliminated by the flowing Ar, and ZnSe solidifies to form the microspheres (as shown in Scheme 1, step I). If the reaction time is short, the obtained products are nearly integrated microspheres without broken holes in the shell. With the prolongation of the deposition time, the SO₂ inside the large ZnSe particles will expand, and the hollow spheres will burst, resulting in an open mouth at the top of each sphere, and the open mouth enlarges as the deposition time increases (as shown in Scheme 1, steps II and III). In addition, in the course of temperature declining, the excessive product particles drop onto the microspheres, so the surfaces of microspheres are not

smooth. With a prolongation reaction time, the particles will fuse together for their lower melting point. The shorter deposition time makes the particles on the surface of the hollow spheres have not enough time to fuse together so the surface of the hollow spheres become smoother and smoother with the prolongation of the deposition time.

To further observe the morphology evolution of the ZnSe hollow microspheres, more experiments were performed. When we reduce the reactants, lower the temperature, and shorten the deposition time, the morphology of the products also changes. Figure 5 shows the SEM images of the products obtained at 1000 °C with different deposition times.

Panels a and b of Figure 5 show the obtained products with a deposition time of 20 min, which clearly shows that the obtained products are sunken hollow microspheres with a diameter of about 3 μm. The formation of the sunken hollow microspheres should be followed as step IV in Scheme 1. We can deduce that the shorter deposition time allows less SO₂ to be trapped inside the ZnSe particles, so the obtained spheres are smaller than those of the products with the long deposition time. The surface of ZnSe hollow microspheres is sunken because of the contractive volume of the gas. In addition, from the images, we can also find that the surface of the microspheres is smoother than those of the products with the long deposition time, for there are only a few excessive product particles produced with a short deposition time.

When we further shorten the deposition time to 10 min, we can obtain ZnSe rings and deflated spheres, as shown in panels c and d of Figure 5. Because of the contractive volume of the gas, in the lowest reactants and deposition time, some of the hollow microspheres are sunken completely from the center to form rings and some of them from different parts of the surface to form complete deflated spheres, which also can be illustrated with step V in Scheme 1. In addition, the diameters of the hollow microspheres are also found to become smaller than those of the previous products. In contrast to former experiments, at the lower temperatures, the volume expansion of gas is reduced, which results in the formation of small hollow microspheres. Table 1 shows the effect of the experimental conditions on the morphology of the final products.

The room temperature PL spectra (Figure 6) from the obtained ZnSe hollow microspheres with different morphologies of complete hollow microspheres, half open mouth hollow microspheres, and broken mouth hollow microspheres have been measured with use of an excitation wavelength of 340 nm.

The emission spectra reveal that the as-prepared ZnSe hollow microspheres of different morphologies have two similar peaks, a blue peak centered at 424 nm and a green emission at 500 nm. The strong emission around 424 nm is usually attributed

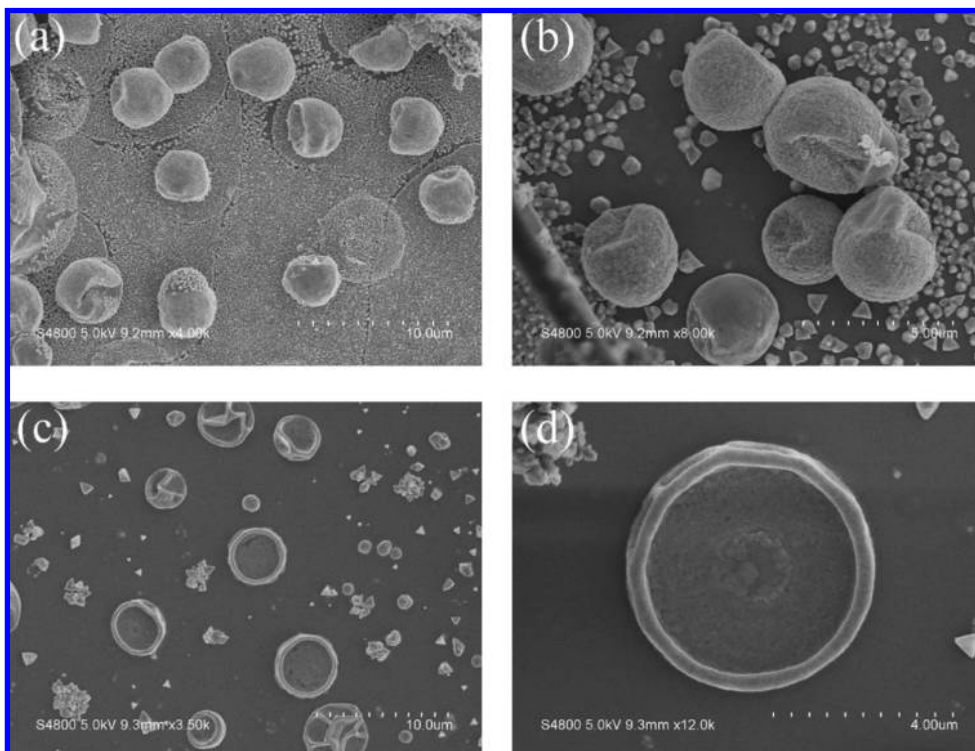
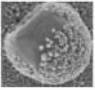
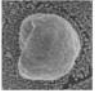
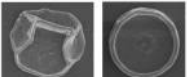


Figure 5. The different morphology of products at 1000 °C: (a and b) different magnification SEM images of sunken hollow microspheres and (c and d) different magnification SEM images of complete deflated spheres.

TABLE 1: The Relationship between Experimental Reaction Conditions and Morphologies

Reactants (g)			Temperature (°C)	Time (min)		Morphologies
ZnS	ZnO	Se		CT[a]	DT[b]	
0.60	0.50	1.20	1000	30	30	
0.40	0.33	0.80	1000	30	20	
0.30	0.25	0.60	1000	30	10	

^a CT: Climbing time. ^b DT: Deposition time.

to the band-edge emission of ZnSe. The weak emission around 500 nm may be assigned to “self-activated” luminescence, probably as a result of some donor–acceptor pairs that are related to Zn vacancy and interstitial states, or associated with dislocations, stacking faults, and nonstoichiometric defects.^{35–38} Comparing the PL spectra of the different morphological ZnSe hollow microspheres, we can find that with a change of the morphology of the hollow microspheres, the absolute and relative intensity of PL is obviously affected. When the deposition time of the ZnSe hollow microspheres become longer, the intensity of the 424 nm emission increases and the relative intensity of the 500 nm emission decreases. The above results should be attributed to the quality of the crystallization of the products. The degree of the crystallization is usually interrelated with the reaction time and temperature. For the complete hollow ZnSe spheres, the deposition time is shortest among the obtained products, which do not have enough time to crystallize completely, and there are many defects in their structures. However, for the broken mouth hollow microspheres, the

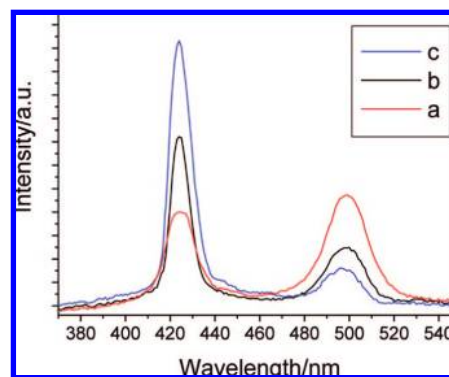


Figure 6. PL spectra of the ZnSe hollow microspheres: (line a) complete hollow microspheres, (line b) half open mouth hollow microspheres, and (line c) broken mouth hollow microspheres.

crystallization time is long enough, so the obtained products are of good quality with fewer defects than those of complete hollow microspheres and half open mouth hollow microspheres. Therefore, the intensity of the band-edge emission increased with the deposition time while the defect emission exhibited the contrary trend. Additionally, the appearance of a peak at 424 nm indicates that ZnSe hollow microspheres may show blue photoluminescence and can potentially be used as blue emitters.

Conclusions

In summary, hollow ZnSe microspheres about 5–15 μm in diameter were prepared successfully by a simple chemistry vapor deposition method in a horizontal tube furnace. The growth mechanism of the ZnSe microspheres can be addressed as SO_2 gas trap, expand, and burst during the deposition process. The evolutions of the morphology of the microspheres are observed. The size, open mouth, surface state, and morphology of the hollow ZnSe microspheres can be adjusted through changing

the experimental conditions. The PL spectra of hollow ZnSe microspheres with different morphologies reveal two similar peaks at 424 and 500 nm. The intensity of the 424 nm emission increases and the relative intensity of the 500 nm decreases with the deposition time. These hollow ZnSe microspheres may have promising applications in blue emitters, gas sensors, microreactors, and catalyst carriers. The method reported here might be exploited to fabricate microspheres of other materials.

Acknowledgment. This work was supported by the National Natural Science Foundation of China (20671003), the Foundation of Key Project of Natural Science of Anhui Education Committee (2006kj041a), and the Education Department of Anhui Province (2006KJ006TD).

References and Notes

- (1) Hines, M. A.; Sionnest, P. G. *J. Phys. Chem. B* **1998**, *102*, 3655.
- (2) Jun, Y. W.; Koo, J. E.; Cheon, J. *Chem. Commun.* **2000**, 1243.
- (3) Quinlan, F. T.; Kuther, J.; Tremel, W.; Knoll, W.; Risbud, S.; Stroeve, P. *Langmuir* **2000**, *16*, 4049.
- (4) Malik, M. A.; Revaprasadu, N.; O'Brien, P. O. *Chem. Mater.* **2001**, *13*, 913.
- (5) Haase, M. A.; Qiu, J.; DePuydt, J. M.; Cheng, H. *Appl. Phys. Lett.* **1991**, *59*, 1272.
- (6) Matasuoka, T. *Adv. Mater.* **1996**, *8*, 469.
- (7) Passler, R.; Griehl, E.; Ripel, H.; Lautner, G.; Bauer, S. *J. Appl. Phys.* **1999**, *86*, 4403.
- (8) Wang, J.; Hutchings, D. C.; Miller, A.; Vanstryland, E. W.; Welford, K. R.; Murhead, I. T.; Lewis, K. L. *J. Appl. Phys.* **1993**, *73*, 4746.
- (9) Hong, S. K.; Kurts, E.; Chang, J. H.; Hanada, T.; Oku, M.; Yao, T. *Appl. Phys. Lett.* **2001**, *78*, 165.
- (10) Li, Q.; Gong, X.; Wang, C.; Wang, J.; Ip, K.; Hark, S. *Adv. Mater.* **2004**, *16*, 1436.
- (11) Zhang, X. T.; Liu, Z.; Leung, Y. P.; Li, Q.; Hark, S. K. *Appl. Phys. Lett.* **2003**, *83*, 5533.
- (12) Chan, Y. F.; Duan, X. F.; Chan, S. K.; Sou, I. K.; Zhang, X. X.; Wang, N. *Appl. Phys. Lett.* **2003**, *83*, 2665.
- (13) Zhang, X. T.; Ip, K. M.; Liu, Z.; Leung, Y. P.; Li, Q.; Hark, S. K. *Appl. Phys. Lett.* **2004**, *84*, 2641.
- (14) Jiang, Y.; Meng, X. M.; Yiu, W. C.; Liu, J.; Ding, J. X.; Lee, C. S.; Lee, S. T. *J. Phys. Chem. B* **2004**, *108*, 2784.
- (15) Hu, J. Q.; Bando, Y.; Golberg, D. *Small* **2005**, *1*, 95.
- (16) Kazes, M.; Lewis, D. Y.; Ebenstein, Y.; Mokari, T.; Banin, U. *Adv. Mater.* **2002**, *14*, 317.
- (17) Lv, R. T.; Cao, C. B.; Zhai, H. Z.; Wang, D. Z.; Liu, S. Y.; Zhu, H. S. *Solid State Commun.* **2004**, *130*, 241.
- (18) Acharya, S.; Panda, A. B.; Efrima, S.; Golan, Y. *Adv. Mater.* **2007**, *19*, 1105.
- (19) Johnson, J. C.; Yan, H. Q.; Schaller, R. D.; Haber, L. H.; Saykally, R. J.; Yang, P. D. *J. Phys. Chem. B* **2001**, *105*, 11387.
- (20) Yang, Y. Y.; Du, F.; Miao, C. *Mater. Lett.* **2008**, *62*, 1334.
- (21) Reiss, P.; Bleuse, J.; Pron, A. *Nano Lett.* **2002**, *2*, 781.
- (22) Morales, M.; Vivet, N.; Levalois, M.; Bardeau, J. F. *Thin Solid Films* **2007**, *515*, 5314.
- (23) Peng, Q.; Dong, Y. J.; Li, Y. D. *Angew. Chem.* **2003**, *115*, 3135; *Angew. Chem., Int. Ed.* **2003**, *42*, 3027.
- (24) Yao, W.; Yu, S. H.; Jiang, J.; Zhang, L. *Chem. Eur. J.* **2006**, *12*, 2066.
- (25) Li, X. L.; Lou, T. J.; Sun, X. M.; Li, Y. D. *Inorg. Chem.* **2004**, *43*, 5442.
- (26) He, T.; Chen, D. R.; Jiao, X. L.; Xu, Y. Y.; Gu, Y. X. *Langmuir* **2004**, *20*, 8404.
- (27) Yin, Y. D.; Lu, Y.; Gates, B.; Xia, Y. N. *Chem. Mater.* **2001**, *13*, 1146.
- (28) Tani, T.; Takatori, K. *J. Am. Chem. Soc.* **2004**, *87*, 523.
- (29) Putlitz, B.; Landfester, K.; Fischer, H.; Antonietti, M.; *Adv. Mater.* **2001**, *13*, 500.
- (30) Nair, A. S.; Tom, R. T.; Suryanarayanan, V.; Pradeep, T. *J. Mater. Chem.* **2003**, *13*, 297.
- (31) Caruso, F.; Spasova, M.; Susha, A.; Giersig, M.; Caruso, R. A. *Chem. Mater.* **2001**, *13*, 109.
- (32) Mayya, K. S.; Gittins, D. I.; Dibaj, A. M.; Caruso, F. *Nano Lett.* **2001**, *1*, 727.
- (33) Wang, L. Z.; Ebina, Y.; Takada, K.; Sasaki, T. *J. Phys. Chem. B* **2004**, *108*, 4283.
- (34) An, X. H.; Meng, G. W.; Wei, Q.; Zhang, X. R.; Hao, Y. F.; Zhang, L. D. *Adv. Mater.* **2005**, *17*, 1783.
- (35) Bukaluk, A.; Trzcinski, M.; Firszt, F.; Legowski, S.; Meczynska, H. *Surf. Sci.* **2002**, *175*, 507.
- (36) Suyver, J. F.; Wuister, S. F.; Kelly, J. J.; Meijerink, A. *Phys. Chem. Chem. Phys.* **2002**, *4*, 5445.
- (37) Zhang, X. B.; Ha, K. L.; Hark, S. K. *Appl. Phys. Lett.* **2001**, *79*, 1127.
- (38) Zhang, X. T.; Liu, Z.; Ip, K. M.; Leung, Y. P.; Li, Q.; Hark, S. K. *J. Appl. Phys.* **2004**, *95*, 5752.

JP803562A